

Stability of periodic orbits in no-slip billiards

C. Cox* R. Feres* H.-K. Zhang†

January 8, 2018

Abstract

Rigid bodies collision maps in dimension two, under a natural set of physical requirements, can be classified into two types: the standard specular reflection map and a second which we call, after Broomhead and Gutkin, *no-slip*. This leads to the study of *no-slip billiards*—planar billiard systems in which the moving particle is a disc (with rotationally symmetric mass distribution) whose translational and rotational velocities can both change at each collision with the boundary of the billiard domain.

In this paper we extend previous results on boundedness of orbits (Broomhead and Gutkin) and linear stability of periodic orbits for a Sinai-type billiard (Wojtkowski) for no-slip billiards. We show among other facts that: (i) for billiard domains in the plane having piecewise smooth boundary and at least one corner of inner angle less than π , no-slip billiard dynamics will always contain elliptic period-2 orbits; (ii) polygonal no-slip billiards always admit small invariant open sets and thus cannot be ergodic with respect to the canonical invariant billiard measure; (iii) the no-slip version of a Sinai billiard must contain linearly stable periodic orbits of period 2 and, more generally, we provide a curvature threshold at which a commonly occurring period-2 orbit shifts from being hyperbolic to being elliptic; (iv) finally, we make a number of observations concerning periodic orbits in a class of polygonal billiards.

1 INTRODUCTION

Consider a billiard dynamical system consisting of a planar domain, referred to as the *billiard table*, and a small disc with rotationally symmetric mass distribution, the *billiard particle*, that slides and rotates freely between successive collisions with the boundary of the table. Upon collision, the particle reflects according to standard mechanics textbook assumptions for conservative rigid body impact to be spelled out shortly. It has long been known that the linear map giving the angular and center of mass velocities immediately after impact in terms of the velocities immediately prior is not uniquely determined; there are exactly two possibilities, each corresponding to a different assumption about the nature of the disc-boundary contact. One possibility represents a perfectly slippery contact that does not create any coupling between translational and angular motion. In this case, by following the center of mass and ignoring rotation, the system reduces to

*Department of Mathematics, Washington University, Campus Box 1146, St. Louis, MO 63130

†Department of Math. & Stat., University of Massachusetts Amherst, MA 01003

the ordinary two-dimensional billiard motion of a point particle with specular reflection, to which most of the literature concerning billiard dynamics is dedicated.

The second possibility represents a perfectly non-slipping contact. This corresponds to a sort of non-dissipative static friction that allows for linear and angular momentum to be partially exchanged at collision. We refer to this type of contact and associated billiards as *no-slip*. They generate a four-dimensional dynamical system (that is to say, the system is generated by the iterations of a map on a four-dimensional energy hypersurface of the billiard phase space) having a number of very distinct properties that are in sharp contrast with ordinary billiard dynamics.

One striking difference has to do with stability of periodic orbits—the main topic of concern of the present paper. A ubiquitous feature of no-slip billiards in dimension 2, which is clearly apparent from numerical simulation, is the presence of elliptic islands near periodic points. As with standard specular billiards [3], these may exist amid chaos created, apparently, by the usual mechanisms of dispersing [15] and focusing [2]. However, in contrast to standard specular billiards (see for example [5] and [6]), this elliptic behavior seems to be very hard to destroy, as the no-slip counterpart to the Sinai billiard will clearly illustrate. It is also apparent from this study that finding ergodic examples of no-slip billiards—one of our initial motivations—is a challenging problem. We note, in passing, that the no-slip billiard map is not symplectic, although it retains some features of symplectic maps. (See Section 5 on measure invariance and reversibility.) On the other hand, the billiard map does preserve the standard Liouville measure and it is time-reversible. The proposed problem of finding ergodic no-slip billiards is for this natural invariant measure.

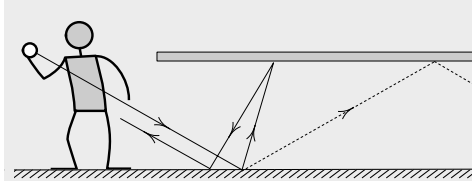


Figure 1: Rendering of Richard L. Garwin’s illustration in his 1969 paper *Kinematics of an Ultraelastic Rough Ball*, in which he introduces the no-slip condition to model the bouncing of a Wham-O Super Ball®.

The no-slip interaction is, naturally (given the above mentioned classification), used whenever rotational effects become important. For example, in [11, 13] the authors apply it to models of transport phenomena in Statistical Mechanics. And in [9], by R.L. Garwin, published in the American Journal of Physics in 1969, the author introduces the no-slip condition to explain how a *super ball* can return to the hand after bouncing against the underside of a table (our Figure 1 reproduces with less charm Figure 1 of his paper). However, very little has been done, to the best of our knowledge, to systematically develop the dynamics and ergodic theory of no-slip planar billiards. Aside from our [7, 8], we know of research by Broomhead and Gutkin [1] showing that no-slip billiard orbits in an

infinite strip are bounded; and by Wojtkowski [19], characterizing linear stability for a special type of period-2 orbit. In the present paper we extend the results in [1] to much more general billiard tables and those of [19] to more general types of periodic orbits.

Detailed statements will be given after a brief review of no-slip billiards, specializing for our present needs basic facts from our [7]. (This reference contains a differential-geometric study classifying rigid bodies collisions in a multidimensional setting.) We only highlight here the following stability result: for a large class of polygonal billiards (which contains all bounded polygons) one can always find elliptic period-2 orbits near which the system is Lyapunov stable. Elliptic period-2 orbits also exist near corners of piecewise smooth billiard shapes with arbitrary curvature, although local (Lyapunov) stability is only shown here when the boundary curvature is zero in a neighborhood of the orbit. It should be recalled in this regard that, different from the dimension-two case in which, by a result of Moser [12], a generic elliptic fixed point of an area-preserving mapping is Lyapunov stable, the same is not true in dimension 4 even for symplectic maps, as shown in [10]. Our Lyapunov stability result depends on an explicit normal-form construction that works so far in zero curvature. It is possible that, using special features of our systems, in particular the fact that they reduce to dimension 3 in a natural way to be explained shortly, one can hope to prove a normal form result also in the variable case. We should note in this regard the comment made in [19] on the possibility of applying KAM-type results for reversible systems such as given in [17, 18]. In any event, we do not resolve this issue here. What we do obtain for the non-flat case are sharp curvature threshold values at which the periodic orbits transition from (linearly) hyperbolic to elliptic, generalizing the main result of [19].

A few remarks are in order concerning notation and visualization. As we are dealing with a four-dimensional system, usefully visualizing the dynamics is less straightforward than for the familiar (slip) planar billiards. By a natural projection, essential features can be described in dimension 3, in what we refer to as the *reduced phase space*, depicted on the left part of Figure 2 (to be explained shortly). The cylinder's cross-sectional disc at height s is the “flattened out” hemisphere of (outgoing) translational-angular velocities of the billiard particle (which are unit vectors in the kinetic energy norm) after colliding with the point on the boundary of the billiard table having arc-length parameter s . In our computer illustrations, we have found it more illuminating to present not the (reduced, three-dimensional) system's phase portrait but the two-dimensional projections shown on the left and right of Figure 3. (The figure shows an orbit segment of the no-slip Sinai billiard, which we investigate in some detail in Section 8.) On the left is the trajectory of the center of mass over the billiard table (the table is suitably shrunk at the margin by the radius of the particle), and on the right is the projection of an orbit from the solid cylinder to the disc. The latter projection will be referred to as a *velocity phase portrait*. It should be kept in mind that velocity portraits depict not a single slice of the cylinder but its entire projection. (We refer the reader to our [8] for many illustrations of velocity portraits for a variety of billiard shapes.)

Concerning notation, a compromise had to be reached between writing linear maps in matrix form in a fixed basis, yielding simpler but maybe more opaque notation, or using a more conceptual, coordinate-free description that imposes greater typographical burden but is much more compact to write. Readers familiar with standard billiard notation

such as used in [4, 16] may not approve of our choice to lean towards the latter (we have in mind especially Section 4), but we believe the alternative would have made the paper longer and more difficult to follow.

The paper is organized as follows. Section 2 introduces the main notations and definitions; Section 3 gives the general description of period-2 orbits; Section 4 expresses the differential of the no-slip billiard map in convenient form for use in the succeeding sections; Section 5 proves invariance of the standard (Liouville) billiard measure and derives a useful consequence from time reversibility of the billiard map; Section 6, which is the technical core of the paper, contains the main stability result for wedge billiards and period-2 orbits; Section 7 extends the main result of the previous section for periodic orbits of general period and gives a classification of periodic orbits on the wedge; Section 8 derives curvature conditions for period-2 orbits to be elliptic; the brief final Section 9 gives a rough conjectural picture of what non-slip billiard dynamics on bounded polygons should look like based on numerical experiments.

2 DEFINITIONS AND BASIC FACTS

Let $\mathcal{B} \subset \mathbb{R}^2$ be a connected region having piecewise smooth boundary, to be referred to as the *billiard table*. Let D denote the disc of radius R in \mathbb{R}^2 centered at the origin. It is given a mass distribution with total mass m whose center of mass coincides with the center of D at 0. We assume that the moment of inertia is finite and denote it by $\mathcal{I} = m(\gamma R)^2$. For the uniform mass distribution, for example, the parameter γ defined by this expression is $\gamma = 1/\sqrt{2}$, and in general $0 \leq \gamma \leq 1$. It is also useful to define $\beta > 0$ such that $\gamma = \tan^2(\beta/2)$. The quantities

$$\cos \beta = \frac{1 - \gamma^2}{1 + \gamma^2}, \quad \sin \beta = \frac{2\gamma}{1 + \gamma^2}$$

will be used throughout the paper. (It will be apparent that when γ is very small and the mass distribution concentrates near the center of the disc, our no-slip billiard systems will approach ordinary planar billiards.)

By a *configuration* of the *billiard particle* D we mean the Euclidean transformation that rotates D by an angle θ and translates the result by an element in \mathcal{B} . It will be convenient to introduce the rotation coordinate $x := \gamma R\theta$. It parametrizes a point (also denoted by x) on the 1-torus $\mathbb{T} := \mathbb{R}/(2\pi\gamma R)$. The 3-dimensional configuration manifold of the billiard system is then $M := \mathcal{B} \times \mathbb{T}$. Points in M will be written as $q = (\bar{q}, x)$. With our choice of x , the kinetic energy of a state (q, v) in the tangent bundle TM is simply $\frac{1}{2}m|v|^2$, where $|v|$ is ordinary Euclidean norm in \mathbb{R}^3 .

Figure 2 illustrates the definition of the (e_1, e_2, e_3) -frame. We focus attention for now on the right-hand side of that figure. (The left-hand side will be explained shortly.) It depicts part of the configuration manifold M and its projection to the billiard table \mathcal{B} . On each $q \in \partial M$ we define the vectors $e_1 = (0, 0, 1)$, the unit vector $e_2(q)$ tangent to $\partial\mathcal{B}$ at q pointing counterclockwise when viewing \mathcal{B} from above (where “up” is set by e_1) and $e_3(q)$, the unit vector perpendicular to $T_q(\partial M)$ pointing into M . These are unit vectors

in the standard Euclidean metric, which is proportional to the Kinetic energy metric (the constant of proportionality is the mass m).

The following subspaces tangent to $\partial M = \partial\mathcal{B} \times \mathbb{T}$ are needed in the definition of the no-slip collision map. Let $q \in \partial M$ and define

$$\mathfrak{S}_q = \{a(-\gamma e_1 + e_2(q)) : a \in \mathbb{R}\}, \quad \bar{\mathfrak{C}}_q = \{a(e_1 + \gamma e_2(q)) : a \in \mathbb{R}\}.$$

Then \mathfrak{S}_q and $\bar{\mathfrak{C}}_q$ are orthogonal subspaces of $T_q(\partial M)$. The *phase space* of the billiard system will be defined as

$$N := N^+ := \{(q, v) \in T\mathbb{R}^3 : q \in \partial M, |v| = 1, v \cdot e_3(q) \geq 0\}.$$

Elements of N are the *post-collision velocities* and elements of $N^- := -N$ are the *pre-collision velocities*. The vector space fiber of N^\pm at q will be denoted N_q^\pm . Thus $v \in N_q^\pm$ if $(q, v) \in N^\pm$. The projection of v to $T_{\bar{q}}\mathcal{B}$ is the center of mass velocity and $v \cdot e_1$ is proportional to angular velocity.

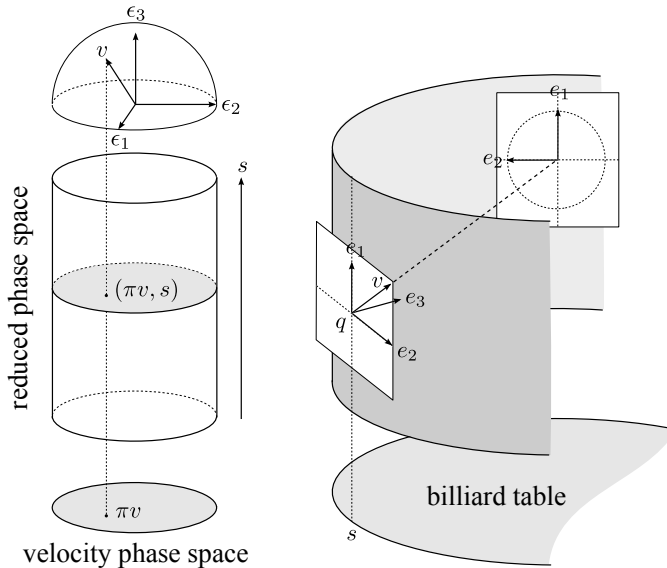


Figure 2: Definition of the product frame (e_1, e_2, e_3) , the reduced phase space, and the velocity phase space. Here πv indicates the orthogonal projection from the hemisphere of unit velocities at q to the disc tangent to ∂M , expressed in the product frame.

By a *collision map* at $q \in \partial M$ we mean a linear map $C_q : T_q M \rightarrow T_q M$ sending N_q^- into N_q . Proposition 1 contains a very special case of the main result of [7], which classifies collision maps for collisions of rigid bodies in \mathbb{R}^n under the following assumptions: energy, translation and angular momenta are conserved, the process is time reversible, and impulse forces between the bodies can only act at the single point of contact. For billiard systems, where one of the bodies (the billiard table) is fixed in place, momentum conservation is

typically void as the group of Euclidean symmetries of the system may be trivial. The last assumption is very strong and, in fact, it generalizes momentum conservation in a sense that is explained in [7].

Proposition 1. *Under the assumptions of energy conservation, time reversibility, and that impulse forces can only act at the point of contact, the collision map C_q sends $e_3(q)$ to its negative, the restriction of C_q to \mathfrak{S}_q is the identity, and its restriction to \mathfrak{C}_q is either plus or minus the identity. The plus sign gives the standard specular reflection map, and the minus sign gives the no-slip map.*

On account of this proposition, the standard (slip) and no-slip billiard reflections seem to have an equal standing as mathematical models of particle collision. As will be noted shortly, however, the system corresponding to the no-slip collision is not Hamiltonian. We speculate that a Hamiltonian model of Garwin's superball behavior would require taking into account more degrees of freedom than a rigid body can have.

For each boundary configuration q let $\sigma_q : \mathbb{R}^3 \rightarrow T_q \mathbb{R}^3$ be the orthogonal map sending the standard basis vectors ϵ_i of \mathbb{R}^3 to $e_i(q)$. Then C_q is represented in the frame (e_1, e_2, e_3) at any q by

$$(1) \quad \mathcal{C} = \sigma_q^{-1} C_q \sigma_q = \begin{pmatrix} -\cos \beta & -\sin \beta & 0 \\ -\sin \beta & \cos \beta & 0 \\ 0 & 0 & -1 \end{pmatrix}.$$

Definition 2 (The no-slip billiard map). *The no-slip billiard map T is the composition of the free motion between two points q_1, q_2 in ∂M and the collision map C_{q_2} at the endpoint. Thus $T : N \rightarrow N$ is given by $(\tilde{q}, \tilde{v}) = T(q, v) = (q + tv, C_{\tilde{q}}v)$ where $t := \inf\{s > 0 : q + sv \in N\}$.*

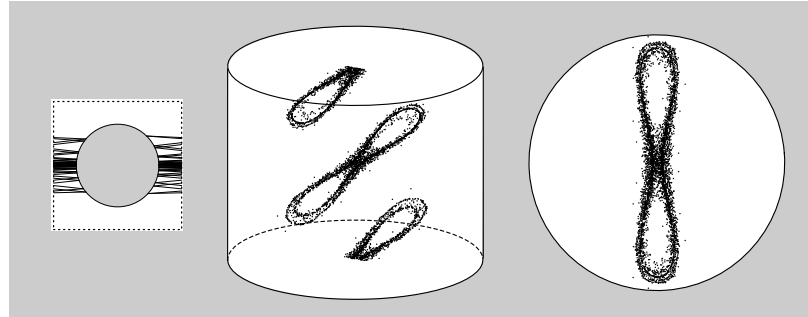


Figure 3: Left: projection from \mathbb{R}^3 to \mathbb{R}^2 of an orbit of the no-slip Sinai billiard, to be discussed in more detail later on. Middle: the same orbit shown in the reduced phase space and, on the right, in the velocity phase space.

Although the notation $T : N \rightarrow N$ suggests that T is defined on all of N , its domain should exclude a set of singular points just as with ordinary billiard maps. Here we

assume that the shape of the billiard table \mathcal{B} is such that T makes sense and is smooth for all ξ in some big subset of N , say open of full Lebesgue measure. This condition will hold for all the billiard domains considered in this paper.

Now let

$$\xi = (q, v) \mapsto \tilde{\xi}_- = (\tilde{q}, v) \mapsto \tilde{\xi} = \tilde{\xi}_+ = (\tilde{q}, C_{\tilde{q}}v).$$

The first map in this composition is parallel translation of v from q to \tilde{q} ; it will be denoted by Φ . The second map, denoted C , applies the no-slip reflection map to the translated vector, still denoted v , at \tilde{q} . Hence $T = C \circ \Phi$.

Taking into account the rotation symmetry of the moving disc, we may for most purposes ignore the angular coordinate (but not the angular velocity!) and restrict attention to the *reduced phase space*. This is defined as $\partial\mathcal{B} \times \{u \in \mathbb{R}^2 : |u| < 1\}$, where an element u of the unit disc represents the velocity vector at $q \in \partial\mathcal{B}$ (pointing into the billiard region) given by

$$\sigma_q(u_1, u_2, \sqrt{1 - |u|^2}) = u_1 e_1(q) + u_2 e_2(q) + \sqrt{1 - |u|^2} e_3(q).$$

By *velocity phase space* we mean this unit disc. Figure 2 summarizes these definitions and Figure 3 shows what an orbit segment looks like in each space for the no-slip Sinai billiard example.

The rotation symmetry that justifies passing from the 4-dimensional phase space to the 3-dimensional reduced phase space may be formally expressed by the identity

$$T(q + \lambda e_1, v) = T(q, v) + \lambda e_1.$$

Note that e_1 is independent of q and that $dT_\xi e_1 = e_1$ for all $\xi = (q, v)$, where dT_ξ is the differential map of T at ξ .

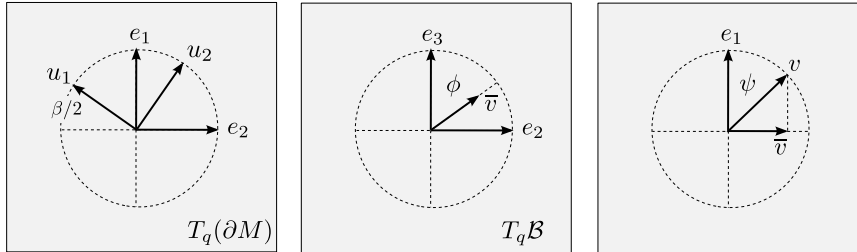


Figure 4: Angle and frame definitions: the q -dependent product frame $(e_i(q))$, the eigenframe $(u_i(q))$ for the collision map C_q at a collision configuration $q \in \partial M$, the characteristic angle β (a function of the mass distribution of the disc), and the angle $\phi(q, v)$ on the plane of the billiard table, and $\psi(q, v)$, on the plane containing e_1 and velocity v .

In addition to $(e_1(q), e_2(q), e_3(q))$ (equivalently, σ_q) it will be useful to introduce a

frame consisting of eigenvectors of the collision map C_q . We define

$$(2) \quad \begin{aligned} u_1(q) &= \sin(\beta/2)e_1(q) - \cos(\beta/2)e_2(q) \\ u_2(q) &= \cos(\beta/2)e_1(q) + \sin(\beta/2)e_2(q) \\ u_3(q) &= e_3(q). \end{aligned}$$

See Figure 4. Then

$$C_q u_1(q) = u_1(q), \quad C_q u_2(q) = -u_2(q), \quad C_q u_3(q) = -u_3(q).$$

Yet a third orthonormal frame will prove useful later on in our analysis of period-2 trajectories. Let $\xi = (q, v) \in N$. Then $w_1(\xi), w_2(\xi), w_3(\xi)$ is the orthonormal frame at q such that

$$w_1(\xi) := \frac{e_1(q) - e_1(q) \cdot vv}{|e_1(q) - e_1(q) \cdot vv|}, \quad w_2(\xi) := v \times w_1(\xi), \quad w_3(\xi) := v.$$

Note that $w_1(\xi)$ and $w_2(\xi)$ span the 2-space perpendicular to v .

Definition 3 (Special orthonormal frames). *For any given $\xi = (q, v) \in N$ we refer to*

$$(e_1(q), e_2(q), e_3(q)), \quad (u_1(q), u_2(q), u_3(q)), \quad (w_1(\xi), w_2(\xi), w_3(\xi))$$

as the product frame, the eigenframe, and the wavefront frame, respectively.

3 PERIOD-2 ORBITS

It appears to be a harder problem in general to show the existence of periodic orbits for no-slip billiards than it is for standard billiard systems in dimension 2, despite numerical evidence that they are very common. A few useful observations can still be made for specific shapes of \mathcal{B} . We begin here with the general description of period-2 orbits. The reader should bear in mind that, when we represent billiard orbits in figures such as 10, we often draw their projections on the plane, even though periodicity refers to a property of orbits in the 3-dimensional reduced phase space.

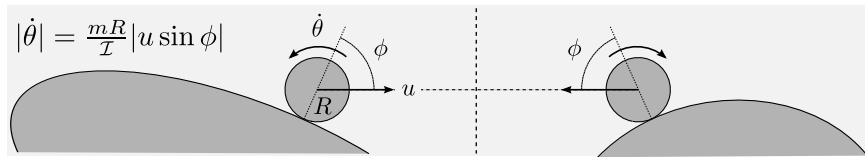


Figure 5: Period 2 orbit. The indicated parameters are: the disc's mass m , its moment of inertia \mathcal{I} , and radius R . The velocity of the center of mass is u and the angular velocity is $\dot{\theta}$.

Let $\xi = (q, v)$ be the initial state of a periodic orbit of period 2, $\tilde{\xi} = (\tilde{q}, \tilde{v}) = T(\xi)$, and t the time of free flight between collisions. Then,

$$(q, v) = (\tilde{q} + tC_{\tilde{q}}v, C_q\tilde{v}) = (q + t(v + C_{\tilde{q}}v), C_qC_{\tilde{q}}v),$$

so that $C_{\tilde{q}}v = -v$ and $v = C_qC_{\tilde{q}}v$. Because v and $u_1(q)$ (respectively, $u_1(\tilde{q})$) are eigenvectors for different eigenvalues of the orthogonal map C_q (respectively, $C_{\tilde{q}}$), v is perpendicular to both $u_1(q)$ and $u_1(\tilde{q})$. It follows from (2) that $u_1(q) \cdot e_1 = u_1(\tilde{q}) \cdot e_1$. Thus the projection of e_1 to v^\perp is proportional to $u_1(q) + u_1(\tilde{q})$. By the definition of the wavefront vector $w_1(\xi)$ (and the angle ϕ , cf. Figure 4) we have

$$w_1(\xi) = w_1(\tilde{\xi}) = \frac{u_1(q) + u_1(\tilde{q})}{|u_1(q) + u_1(\tilde{q})|} = \frac{u_1(q) + u_1(\tilde{q})}{2\sqrt{1 - \cos^2(\beta/2)\cos^2\phi}}.$$

Now observe that $u_1(\tilde{q}) - u_1(q)$ is perpendicular to $u_1(q) + u_1(\tilde{q})$. It follows from this remark and a glance at Figure 4 (to determine the orientation of the vectors) that

$$w_2(\xi) = -w_2(\tilde{\xi}) = \frac{u_1(\tilde{q}) - u_1(q)}{|u_1(\tilde{q}) - u_1(q)|} = \frac{u_1(\tilde{q}) - u_1(q)}{2\cos(\beta/2)\cos\phi}.$$

Notice, in particular, that v is a positive multiple of $u_1(q) \times u_1(\tilde{q})$. An elementary calculation starting from this last observation gives v in terms of the product frame:

$$v = \frac{\cos(\beta/2)\sin\phi e_1 + \sin(\beta/2)[\sin\phi e_2(q) + \cos\phi e_3(q)]}{\sqrt{1 - \cos^2(\beta/2)\cos^2\phi}}.$$

A more physical description of the velocity v of a period-2 orbit is shown in Figure 5 in terms of the moment of inertia \mathcal{J} .

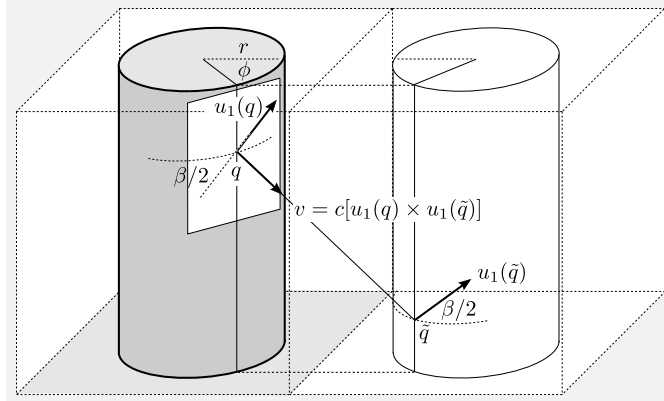


Figure 6: Two fundamental domains of the no-slip Sinai billiard and an initial velocity v of a periodic orbit with period 2. This trajectory lies in a one-parameter family of period-2 trajectories parametrized by the angle ϕ .

Equally elementary computations yield the collision map C_q in the wavefront frame at q , for a period-2 state $\xi = (q, v)$. We register this here for later use. To shorten the

equations we write $c_{\beta/2} = \cos(\beta/2)$ and $c_\phi = \cos \phi$.

$$(3) \quad \begin{aligned} C_q w_1(\xi) &= (1 - 2c_{\beta/2}^2 c_\phi^2) w_1(\xi) - 2c_{\beta/2} c_\phi \sqrt{1 - c_{\beta/2}^2 c_\phi^2} w_2(\xi) \\ C_q w_2(\xi) &= -2c_{\beta/2} c_\phi \sqrt{1 - c_{\beta/2}^2 c_\phi^2} w_1(\xi) - (1 - 2c_{\beta/2}^2 c_\phi^2) w_2(\xi) \\ C_q w_3(\xi) &= -w_3(\xi). \end{aligned}$$

The following easily obtained inner products will also be needed later.

$$(4) \quad \begin{aligned} u_1(\tilde{q}) \cdot u_1(q) &= 1 - 2 \cos^2(\beta/2) \cos^2 \phi \\ w_1(\xi) \cdot u_1(q) &= \sqrt{1 - \cos^2(\beta/2) \cos^2 \phi} \\ w_2(\xi) \cdot u_1(q) &= -\cos(\beta/2) \cos \phi. \end{aligned}$$

Figure 6 shows (two copies of the fundamental domain of) the configuration manifold of the no-slip Sinai billiard. Here the billiard table is the complement of a circular scatterer in a two-dimensional torus and M is the cartesian product of the latter with a one-dimensional torus. Notice that there is a whole one-parameter family of initial conditions giving period-2 orbits, parametrized by the angle ϕ . We obtain infinitely many such families by choosing different pairs of fundamental domains. (Figure 3 is also about this system.) We will return to the no-slip Sinai billiard in Section 8.

4 THE DIFFERENTIAL OF THE NO-SLIP BILLIARD MAP

Mostly, in this section, we write $\langle u, v \rangle$ instead of $u \cdot v$ for the standard inner product of \mathbb{R}^3 . Let $q(s)$ be a smooth curve in ∂M such that $q(0) = q$ and $q'(0) = X \in T_q(\partial M)$. Define

$$\omega_q(X) := \frac{d}{ds} \Big|_{s=0} \sigma(q(0))^{-1} \sigma(q(s)) \in \mathfrak{so}(3),$$

where $\mathfrak{so}(3)$ is the space of antisymmetric 3×3 matrices (the Lie algebra of the rotation group) and $\sigma(q) := \sigma_q$ is the product frame. As the field e_1 is constant and $\omega_q(X)$ is antisymmetric we have $\omega_q(X)_{ij} = 0$ except possibly for $(i, j) = (2, 3)$ and $(3, 2)$. Denoting by D_X directional derivative of vector fields along X at q ,

$$\omega_q(X)_{23} = \epsilon_2 \cdot \left[\frac{d}{ds} \Big|_{s=0} \sigma(q(0))^{-1} \sigma(q(s)) \epsilon_3 \right] = \langle e_2(q), D_X e_3 \rangle = \langle e_2(q), X \rangle \langle e_2(q), D_{e_2(q)} e_3 \rangle$$

since $D_{e_1} e_3 = 0$. The inner product $\kappa(q) := \langle e_2(q), D_{e_2(q)} e_3 \rangle$ is the geodesic curvature of the boundary of \mathcal{B} at \bar{q} , where \bar{q} is the base point of q in $\partial \mathcal{B}$. Thus

$$(5) \quad \omega_q(X) = \kappa(q) \langle e_2(q), X \rangle \mathcal{A},$$

where

$$\mathcal{A} = \begin{pmatrix} 0 & 0 & 0 \\ 0 & 0 & 1 \\ 0 & -1 & 0 \end{pmatrix}.$$

Given vector fields μ, ν , it is convenient to define $\mu \odot \nu$ as the map

$$(6) \quad (q, v) \mapsto (\mu \odot \nu)_q v := \langle \mu_q, v \rangle \nu_q + \langle \nu_q, v \rangle \mu_q.$$

Lemma 4. *The directional derivative of C along $X \in T_q(\partial M)$ is*

$$D_X C = \kappa(q) \langle e_2(q), X \rangle \mathcal{O}_q,$$

where $\mathcal{O}_q := \sigma_q \mathcal{O} \sigma_q^{-1}$, \mathcal{O} is the commutator of \mathcal{A} and \mathcal{C} given by

$$\mathcal{O} := \mathcal{A}\mathcal{C} - \mathcal{C}\mathcal{A} = 2\cos(\beta/2) \begin{pmatrix} 0 & 0 & \sin(\beta/2) \\ 0 & 0 & -\cos(\beta/2) \\ \sin(\beta/2) & -\cos(\beta/2) & 0 \end{pmatrix}$$

and \mathcal{C} was defined above in (1). Furthermore, $\mathcal{O}_q = 2\cos(\beta/2)(u_1 \odot e_3)_q$ and

$$D_X C = 2\cos(\beta/2)\kappa(q)\langle X, e_2 \rangle_q (u_1 \odot e_3)_q.$$

Proof. Notice that $0 = D_X I = D_X(\sigma^{-1}\sigma) = (D_X\sigma^{-1})\sigma + \sigma^{-1}D_X\sigma$. Thus

$$D_X\sigma^{-1} = -\sigma^{-1}(D_X\sigma)\sigma^{-1}.$$

Therefore,

$$D_X C = (D_X\sigma)\mathcal{C}\sigma^{-1} + \sigma\mathcal{C}D_X\sigma^{-1} = \sigma[\sigma^{-1}D_X\sigma]\mathcal{C}\sigma^{-1} - \sigma\mathcal{C}[\sigma^{-1}D_X\sigma]\sigma^{-1} = \sigma[\omega(X), \mathcal{C}]\sigma^{-1}.$$

The first claimed expression for $D_X C$ is now a consequence of Equation 5. A simple computation also gives, for any given $v \in \mathbb{R}^3$,

$$(7) \quad \mathcal{O}_q v = 2\cos(\beta/2)(e_3 \odot u_1)_q v,$$

yielding the second expression for $D_X C$. \square

It is also convenient to define the following two projections. Let $\xi = (q, v) \in N^\pm$. The space $T_\xi N^\pm$ decomposes as a direct sum $T_\xi N^\pm = H_\xi \oplus V_\xi$ where

$$H_\xi = T_q N = \{X \in \mathbb{R}^3 : X \cdot e_3(q) = 0\} \text{ and } V_\xi = v^\perp = \{Y \in \mathbb{R}^3 : Y \cdot v = 0\}.$$

(Recall that $N := N^+$.) We refer to these as the *horizontal* and *vertical* subspaces of $T_\xi N^\pm$. We use the same symbols to denote the projections $H_\xi : \mathbb{R}^3 \rightarrow T_q(\partial M)$ and $V_\xi : \mathbb{R}^3 \rightarrow v^\perp$ defined by

$$H_\xi Z := Z - \frac{\langle Z, e_3(q) \rangle}{\langle v, e_3(q) \rangle} v, \quad V_\xi Z := Z - \langle Z, v \rangle v.$$

We note that for $\xi = (q, v) \in N^\pm$ and $Z \in \mathbb{R}^3$

$$\langle e_2(q), H_\xi Z \rangle = \frac{\langle Z, e_2(q) \rangle \langle v, e_3(q) \rangle - \langle Z, e_3(q) \rangle \langle v, e_2(q) \rangle}{\langle v, e_3(q) \rangle} = \frac{\langle v \times e_1(q), Z \rangle}{\langle v, e_3(q) \rangle}.$$

Also observe that $v \times e_1 = |\bar{v}|w_2(\xi)$, where w_2 is the second vector in the wavefront frame (cf. Definition 3) and \bar{v} is the orthogonal projection of v to the plane perpendicular to e_1 . Thus, denoting by $\phi(\xi)$ the angle between \bar{v} and $e_3(q)$ (this is the same ϕ as in Figures 4, 5 and 6)

$$(8) \quad \langle e_2(q), H_\xi Z \rangle = \frac{1}{\cos \phi(\xi)} \langle w_2(\xi), Z \rangle.$$

Let $q \in \partial M$, $v = v_- \in N_q^-$, $v_+ := C_q v_- \in N_q^+$, $\xi = \xi_- = (q, v_-)$, $\xi_+ = (q, v_+)$. Define

$$(9) \quad \Lambda_\xi := V_{\xi_+} H_{\xi_-} : v_-^\perp \rightarrow v_+^\perp.$$

Clearly Λ_ξ is defined on all of \mathbb{R}^3 , not only on v_-^\perp , but we are particularly interested in its restriction to the latter subspace.

Let $\xi = (q, v)$ be a point contained in a neighborhood of N where T is defined and differentiable. Set $\tilde{\xi} = T(\xi)$. We wish to describe $dT_\xi : T_\xi N \rightarrow T_{\tilde{\xi}} N$. Let $\xi(s) = (q(s), v(s))$ be a differentiable curve in N with $\xi(0) = \xi$ and define

$$X := q'(0) \in T_q N, \quad Y := v'(0) \in v^\perp.$$

Then $\tilde{\xi}(s) = T(\xi(s)) = (\tilde{q}(s), \tilde{v}(s)) \in N$ where $\tilde{q}(s) = q(s) + t(s)v(s)$ and $\tilde{v}(s) = C_{\tilde{q}(s)}v(s)$. From the equality $\langle \tilde{q}'(0), e_3(\tilde{q}) \rangle = 0$ it follows that

$$t'(0) = -\frac{\langle X + tY, e_3(\tilde{q}) \rangle}{\langle v, e_3(\tilde{q}) \rangle}.$$

Consequently, $\tilde{X} := \tilde{q}'(0) \in T_{\tilde{q}} N$ and $\tilde{Y} := \tilde{v}'(0) \in \tilde{v}^\perp$ satisfy

$$\tilde{X} = X + tY - \frac{\langle X + tY, e_3(\tilde{q}) \rangle}{\langle v, e_3(\tilde{q}) \rangle} v = H_{\tilde{\xi}_-}(X + tY)$$

and

$$\tilde{Y} = C_{\tilde{q}} Y + \left[\frac{d}{ds} \Big|_{s=0} C_{\tilde{q}(s)} \right] v = C_{\tilde{q}} Y + \kappa(\tilde{q}) \langle e_2(\tilde{q}), \tilde{X} \rangle \mathcal{O}_{\tilde{q}} v,$$

where we have used Lemma 4. From the same lemma, $\mathcal{O}_q v = -2 \cos(\beta/2) (\nu \odot u_1)_{\tilde{q}} v$. Thus

$$(10) \quad \begin{aligned} \tilde{X} &= H_{\tilde{\xi}_-}(X + tY) \\ \tilde{Y} &= C_{\tilde{q}} Y - 2 \cos(\beta/2) \kappa(\tilde{q}) \langle e_2(\tilde{q}), H_{\tilde{\xi}_-}(X + tY) \rangle (\nu \odot u_1)_{\tilde{q}} v. \end{aligned}$$

As already noted, $T_\xi N^+ = T_q(\partial M) \oplus v^\perp$. By using the projection $V_\xi : T_q(\partial M) \rightarrow v^\perp$ introduced earlier we may identify $T_\xi N^+$ with the sum $v^\perp \oplus v^\perp$. In this way dT_ξ is regarded as a map from $v^\perp \oplus v^\perp$ to $\tilde{v}^\perp \oplus \tilde{v}^\perp$.

Proposition 5. *Let $T : N \rightarrow N$ be the billiard map, $\xi = (q, v) \in N$ and $(\tilde{q}, \tilde{v}) = \tilde{\xi} = T(\xi)$, where $\tilde{q} = q + tv$, and $\tilde{v} = C_{\tilde{q}} v$. Under the identification of the tangent space $T_\xi N$ with $v^\perp \oplus v^\perp$ as indicated just above, we may regard the differential dT_ξ as a linear map from $v^\perp \oplus v^\perp$ to $\tilde{v}^\perp \oplus \tilde{v}^\perp$. Also recall from (8) the definition of $\Lambda_{\tilde{\xi}} : v^\perp \rightarrow \tilde{v}^\perp$. Then $dT_\xi : T_\xi N \rightarrow T_{\tilde{\xi}} N$ is given by*

$$\begin{pmatrix} X \\ Y \end{pmatrix} \mapsto \begin{pmatrix} \Lambda_{\tilde{\xi}}(X + tY) \\ C_{\tilde{q}} Y + 2 \cos(\beta/2) \kappa(\tilde{q}) \frac{\langle e_3 \odot u_1 \rangle_{\tilde{q}} v}{\cos \phi(\tilde{q}, v)} \langle w_2(\xi), X + tY \rangle \end{pmatrix},$$

where $\cos \phi(\tilde{q}, v) = \langle \bar{v}/|\bar{v}|, e_3(\tilde{q}) \rangle$ and \bar{v} is the orthogonal projection of v to e_1^\perp .

Proof. This is a consequence of the preceding remarks and definitions. \square

Corollary 6. *If $\xi = (q, v)$ is periodic of period 2, then $C_{\tilde{q}}v = -v$, $\langle v, u_1(\tilde{q}) \rangle = 0$, and the map of Proposition 5 reduces to*

$$\begin{pmatrix} X \\ Y \end{pmatrix} \mapsto \begin{pmatrix} X + tY \\ C_{\tilde{q}}Y + 2 \cos(\beta/2) \kappa(\tilde{q}) \frac{\cos \psi(\tilde{q}, v)}{\cos \phi(\tilde{q}, v)} \langle w_2(\xi), X + tY \rangle u_1(\tilde{q}) \end{pmatrix}.$$

where $\cos \psi(\tilde{q}, v) := \langle v, e_3(\tilde{q}) \rangle$, $\cos \phi(\tilde{q}, v) = \langle \bar{v}/|\bar{v}|, e_3(\tilde{q}) \rangle$.

Proof. Clearly, $C_{\tilde{q}}v = -v$, whence $\langle v, u_1(\tilde{q}) \rangle = 0$ and $(e_3 \odot u_1)_{\tilde{q}}v = \langle e_3(\tilde{q}), v \rangle u_1(\tilde{q})$. Also notice that $\Lambda_{\tilde{\xi}}Z = Z$ whenever $\langle Z, v \rangle = 0$. The corollary follows. \square

5 MEASURE INVARIANCE AND TIME REVERSIBILITY

It will be seen below that the no-slip billiard map does not preserve the natural symplectic form on N , so these systems are not Hamiltonian. Nevertheless, the canonical billiard measure derived from the symplectic form (the Liouville measure) is invariant and the system is time reversible, so some of the good features of Hamiltonian systems are still present. (See, for example, [17, 18] where a KAM theory is developed for reversible systems.)

Recall that an invertible map T is said to be *reversible* if there exists an involution \mathcal{R} such that

$$\mathcal{R} \circ T \circ \mathcal{R} = T^{-1}.$$

In order to see that the no-slip billiard map T is reversible we first define the following maps: $\Phi : (q, v) \mapsto (q+tv, v)$, where t is the time of free motion of the trajectory with initial state (q, v) , so that $q, q+tv \in \partial M$; the collision map $C : N \rightarrow N$ given by $C(q, v) = (q, C_q v)$; and the flip map $J : (q, v) \mapsto (q, -v)$ where $q \in \partial M$ and $v \in \mathbb{R}^3$. Recall that $T = C \circ \Phi$. Now set $\mathcal{R} := J \circ C = C \circ J$. It is clear (since C_q is an involution by Proposition 1) that $\mathcal{R}^2 = I$ and that $J \circ \Phi \circ J = \Phi^{-1}$. Therefore,

$$\mathcal{R} \circ T \circ \mathcal{R} = J \circ C^2 \circ \Phi \circ J \circ C = J \circ \Phi \circ J \circ C = \Phi^{-1} \circ C = (C \circ \Phi)^{-1} = T^{-1}.$$

Notice that if $L : V \rightarrow V$ is a reversible isomorphism of a vector space V with time reversal map $\mathcal{R} : V \rightarrow V$ (so that $\mathcal{R} \circ L \circ \mathcal{R} = L^{-1}$) then for any eigenvalue λ of L associated to eigenvector u , $1/\lambda$ is also an eigenvalue for the eigenvector $\mathcal{R}u$, as easily checked. These elementary observations have the following useful corollary.

Proposition 7. *Let $\xi \in N$ be a periodic point of period k of the no-slip billiard system and let λ be an eigenvalue of the differential map $dT_{\xi}^k : T_{\xi}N \rightarrow T_{\xi}N$ corresponding to eigenvector u . Then $1/\lambda$ is also an eigenvalue of dT_{ξ}^k corresponding to eigenvector $\mathcal{R}u$, where \mathcal{R} is the composition of the collision map C and the flip map J . Furthermore, e_1 (see Definition 3) is always an eigenvector of dT_{ξ} and all its powers, corresponding to the eigenvalue 1.*

We now turn to invariance of the canonical measure. The canonical 1-form θ on N is defined by

$$\theta_{\xi}(U) := v \cdot X$$

for $\xi = (q, v) \in N$ and $U = (X, Y) \in T_q N \oplus v^\perp = T_\xi N$. Its differential $d\theta$ is a symplectic form on $N \cap \{v \in T_q(\partial M) : |v| = 1\}^c$ and $\Omega = d\theta \wedge d\theta$ is the canonical volume form on this same set. In terms of horizontal and vertical components of vectors in TN , the symplectic form is expressed as

$$d\theta(U_1, U_2) = Y_1 \cdot X_2 - Y_2 \cdot X_1,$$

where $U_i = (X_i, Y_i)$. An elementary computation shows that the measure on N associated to Ω is given by

$$(11) \quad |\Omega_\xi| = v \cdot \nu(q) dA_{\partial M}(q) dA_N(v),$$

where $\nu(q) := e_3(q)$, $dA_{\partial M}(q)$ is the area measure on ∂M , and $dA_N(v)$ is the area measure on the hemisphere $N_q = \{v \in \mathbb{R}^3 : v \cdot \nu(q) > 0\}$.

Proposition 8. *The canonical 4-form Ω on N transforms under the no-slip billiard map as $T^*\Omega = -\Omega$. In particular, the associated measure $|\Omega|$, shown explicitly in Equation (11), is invariant under T .*

Proof. Let u be a vector field on ∂M and introduce the one-form θ^u on N given by

$$\theta_\xi^u(U) := (v \cdot u(q))(u(q) \cdot X)$$

for $\xi = (q, v)$ and $U = (X, Y)$. Taking u to be each of the vector fields u_1, u_2 we obtain the 1-forms θ^{u_1} and θ^{u_2} . As $v = (v \cdot u_1)u_1 + (v \cdot u_2)u_2 + (v \cdot \nu)\nu$ and $X \cdot \nu = 0$, we have

$$\theta = \theta^{u_1} + \theta^{u_2}.$$

The no-slip collision map C acts on $u = \theta^{u_i}$ as follows: For $U = (X, Y) \in T_q(\partial M) \oplus v^\perp$,

$$(C^*\theta^u)_\xi(U) = (C_q(v) \cdot u(q))(u(q) \cdot X) = (v \cdot C_q(u(q)))(u(q) \cdot X),$$

where C^* denotes the pull-back operation on forms. It follows that

$$C^*\theta^{u_1} = \theta^{u_1}, \quad C^*\theta^{u_2} = -\theta^{u_2}.$$

We now compute the differentials $d\theta^u$ for $u = u_1, u_2$. Observe that $\theta^u = f^u(\xi)(\pi^*u^\flat)$, where f^ξ is the function on N defined by $f^u(\xi) := v \cdot u(q)$ and π^*u^\flat is the pull-back under the projection map $\pi : N \rightarrow \partial M$ of the 1-form u^\flat on ∂M given by $u_q^\beta(X) = u(q) \cdot X$. Thus

$$d\theta^u = df^u \wedge (\pi^*u^\flat) + f^u \pi^* du^\flat.$$

A simple calculation gives

$$df_\xi^u(X, Y) = v \cdot (D_X u) + u(q) \cdot Y.$$

The vector field $u = u_i$ is parallel on ∂M . In fact, its derivative in direction $X \in T_q(\partial M)$ only has component in the normal direction, given by

$$D_X u = \kappa(q)(X \cdot e_2(q))(u(q) \cdot e_2(q))\nu(q).$$

Omitting the dependence on q , we have

$$df_\xi^u(X, Y) = \kappa(q)(X \cdot e_2)(u \cdot e_2)(v \cdot \nu) + u \cdot Y.$$

Another simple calculation gives

$$du_q^\flat(X_1, X_2) = (D_{X_1}u) \cdot X_2 - (D_{X_2}u) \cdot X_1 = 0,$$

so $d\theta^u = df^u \wedge \pi^*u^\flat$. Explicitly,

$$d\theta^u(U_1, U_2) = (u \cdot Y_1)(u \cdot X_2) - (u \cdot Y_2)(u \cdot X_1) - \kappa(q)(v \cdot \nu)(u \cdot e_1)(u \cdot e_2)\omega(X_1, X_2),$$

where

$$\omega(X_1, X_2) := (e_1 \cdot X_1)(e_2 \cdot X_2) - (e_2 \cdot X_1)(e_1 \cdot X_2).$$

Notice that ω is the area form on ∂M . A convenient way to express $d\theta^u$ is as follows. Define the 1-form \tilde{u} on N by $\tilde{u}_\xi(U) = u(q) \cdot Y$, where $U = (X, Y) \in T_\xi N$, and the function $g^u(\xi) := -\kappa(q)(v \cdot \nu)(u \cdot e_1)(u \cdot e_2)$. These extra bits of notation now allow us to write

$$d\theta_\xi^u = g^u(\xi)(\pi^*\omega) + \tilde{u} \wedge (\pi^*u^\flat).$$

The main conclusion we wish to derive from these observations is that $d\theta^u \wedge d\theta^u = 0$. This is the case because, as $\dim(\partial M) = 2$, we must have $\omega^2 = 0$ and $\omega \wedge u^\flat = 0$. Therefore,

$$\Omega := d\theta \wedge d\theta = (d\theta^{u_1} + d\theta^{u_2}) \wedge (d\theta^{u_1} + d\theta^{u_2}) = 2d\theta^{u_1} \wedge d\theta^{u_2}.$$

Finally,

$$C^*\Omega = 2d(C^*\theta^{u_1}) \wedge d(C^*\theta^{u_2}) = -2d\theta^{u_1} \wedge d\theta^{u_2} = -\Omega.$$

The forms $d\theta$ and Ω are invariant under the geodesic flow and under the map it induces on N . As T is the composition of this map and C , the proposition is established. \square

6 WEDGE BILLIARDS

One of the main observations of this paper is that a wedge billiard (as in Figure 7) always contains, arbitrarily near its corner, period-2 orbits which are Lyapunov stable. This then implies the existence of such stable orbits for most polygonal billiards. This is proved in the present section.

We set the following conventions for a wedge table with corner angle 2ϕ . See Figure 7. (This is the same ϕ that has appeared before in previous figures.) The boundary planes of the configuration manifold are denoted \mathcal{P}_1 and \mathcal{P}_2 . The orthonormal vectors of the constant product frame on plane \mathcal{P}_i are $e_{1,i}, e_{2,i}, e_{3,i} = \nu_i$ for $i = 1, 2$ where

$$e_{1,1} = \begin{pmatrix} 0 \\ 0 \\ 1 \end{pmatrix}, \quad e_{2,1} = \begin{pmatrix} \cos \phi \\ -\sin \phi \\ 0 \end{pmatrix}, \quad e_{3,1} = \begin{pmatrix} \sin \phi \\ \cos \phi \\ 0 \end{pmatrix},$$

$$e_{1,2} = \begin{pmatrix} 0 \\ 0 \\ 1 \end{pmatrix}, \quad e_{2,2} = -\begin{pmatrix} \cos \phi \\ \sin \phi \\ 0 \end{pmatrix}, \quad e_{3,2} = \begin{pmatrix} \sin \phi \\ -\cos \phi \\ 0 \end{pmatrix}.$$

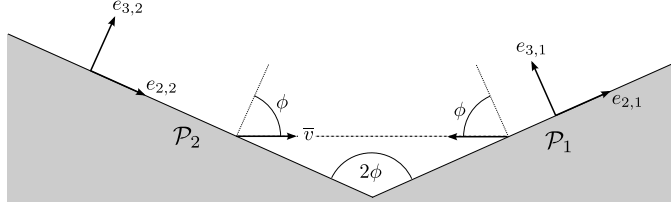


Figure 7: Some notation specific to the wedge billiard table. The \mathcal{P}_i are the half-plane components of the boundary of the configuration manifold.

Let $\sigma_i : \mathbb{R}^3 \rightarrow T_q \oplus \mathbb{R}\nu_i$ be the constant orthogonal map such that $\sigma_i \epsilon_j = e_{j,i}$, where ϵ_i , $i = 1, 2, 3$, is our notation for the standard basis vectors in \mathbb{R}^3 . Let

$$u_{1,i} = \sin(\beta/2)e_{1,i} - \cos(\beta/2)e_{2,i}, \quad u_{2,i} = \cos(\beta/2)e_{1,i} + \sin(\beta/2)e_{2,i}, \quad u_{3,i} = e_{3,i} = \nu_i$$

be the eigenvectors of the no-slip reflection map associated to the plane \mathcal{P}_i and set $\zeta_i \epsilon_j := u_{j,i}$. For easy reference we record their matrices here:

$$\zeta_i = \begin{pmatrix} (-1)^i \cos(\beta/2) \cos \phi & -(-1)^i \sin(\beta/2) \cos \phi & \sin \phi \\ \cos(\beta/2) \sin \phi & -\sin(\beta/2) \sin \phi & -(-1)^i \cos \phi \\ \sin(\beta/2) & \cos(\beta/2) & 0 \end{pmatrix}.$$

The initial velocity v for the period-2 trajectory points in the direction of $u_{1,2} \times u_{1,1}$ and is given by

$$v = \frac{1}{\sqrt{1 - \cos^2(\beta/2) \cos^2 \phi}} \begin{pmatrix} 0 \\ \sin(\beta/2) \\ \cos(\beta/2) \sin \phi \end{pmatrix}.$$

This periodic trajectory connects the points $q_1 \in \mathcal{P}_1$ and $q_2 \in \mathcal{P}_2$. Any such pair of points can be written as

$$q_1 = a \begin{pmatrix} \sin(\beta/2) \cos \phi \\ -\sin(\beta/2) \sin \phi \\ b - \cos(\beta/2) \sin^2 \phi \end{pmatrix}, \quad q_2 = a \begin{pmatrix} \sin(\beta/2) \cos \phi \\ \sin(\beta/2) \sin \phi \\ b + \cos(\beta/2) \sin^2 \phi \end{pmatrix},$$

where $a, b \in \mathbb{R}$, $a > 0$. In what follows we assume without loss of generality that $a = 1$ and $b = 0$. Thus

$$q_i = (\sin(\beta/2) \cos \phi, (-1)^i \sin(\beta/2) \sin \phi, (-1)^i \cos(\beta/2) \sin^2 \phi)^t.$$

Let $S_i^\pm = \{v \in \mathbb{R}^3 : |v| = 1, \pm v \cdot \nu_i > 0\}$. The collision maps $C_i : S_i^- \rightarrow S_i^+$, $i = 1, 2$ are given by the matrices

$$C_i = \sigma_i \mathcal{C} \sigma_i^{-1} = \zeta_i \begin{pmatrix} 1 & 0 & 0 \\ 0 & -1 & 0 \\ 0 & 0 & -1 \end{pmatrix} \zeta_i^{-1},$$

where \mathcal{C} was defined in Equation (1). We now introduce coordinates on $\mathcal{P}_i \times S_i^+$ as follows. Let $S_+^2 = \{z \in \mathbb{R}^3 : |z| = 1, z_3 > 0\}$ and define $\Phi_i : \mathbb{R}^2 \times S_+^2 \rightarrow \mathcal{P}_i \times S_i^+$ by

$$\Phi_i(x, y) = (q_i + x_1 u_{1,i} + x_2 u_{2,i}, y_1 u_{1,i} + y_2 u_{2,i} + y_3 u_{3,i}).$$

Regarding $x \in \mathbb{R}^2$ as $(x, 0) \in \mathbb{R}^3$, we may then write

$$\Phi_i(x, y) = (q_i + \zeta_i x, \zeta_i y).$$

Clearly, the billiard map is not defined on all of $\bigcup_i \mathcal{P}_i \times S_i^+$ since those initial velocities not pointing towards the other plane will escape to infinity, but we are interested in the behavior of the map on a neighborhood of the periodic point $\xi_i = (q_i, v_i)$, $v_i = -(-1)^i v$. The question of interest here is whether some open neighborhood of ξ_i remains invariant under the billiard map. It is easily shown that the coordinates of the state ξ_i (of the period-2 orbit at the plane \mathcal{P}_i) are $\Phi_i^{-1}(\xi_i) = (0, y_i) \in \mathbb{R}^2 \times S_+^2$ where

$$y_i = \frac{1}{\sqrt{1 - \cos^2(\beta/2) \cos^2 \phi}} (0, (-1)^i \sin \phi, \sin(\beta/2) \cos \phi)^t.$$

Let $T_i : \mathcal{D}_i \subset \mathbb{R}^2 \times S_+^2 \rightarrow \mathbb{R}^2 \times S_+^2$ be the billiard map restricted to $\mathcal{P}_i \times S_i^+$ expressed in the coordinate system defined by Φ_i . Thus

$$T_1 = \Phi_2^{-1} T \Phi_1, \quad T_2 = \Phi_1^{-1} T \Phi_2$$

on their domains \mathcal{D}_i . We now find the explicit form of T_i . Define $\bar{i} = \begin{cases} 1 & \text{if } i = 2 \\ 2 & \text{if } i = 1 \end{cases}$ and orthogonal matrices $A_i := \zeta_i^{-1} \zeta_{\bar{i}}$ and $S = \text{diag}(1, -1, -1)$, both in $SO(3)$. Also define

$$\alpha := 2 \sin \phi \sqrt{1 - \cos^2(\beta/2) \cos^2 \phi}.$$

Observe that $\zeta_{\bar{i}}^{-1} C_{\bar{i}} \zeta_i = S A_i$. It is easily shown that

$$q_i - q_{\bar{i}} = -\alpha v_i, \quad v_i = \zeta_i y_i, \quad A_i y_i = -y_{\bar{i}}, \quad S A_i y_i = y_{\bar{i}}.$$

In particular, $\zeta_{\bar{i}}^{-1} (q_i - q_{\bar{i}}) = -\alpha y_i$. Let $Q : \mathbb{R}^3 \times S_+^2 \rightarrow \mathbb{R}^2$ be defined by

$$Q(x, y) := x - \frac{x \cdot \epsilon_3}{y \cdot \epsilon_3} y.$$

Notice that $Q(x, y) \cdot \epsilon_3 = 0$. We now have

$$(12) \quad T_i : (x, y) \mapsto (Q(A_i(x - \gamma y_i), A_i y_i), S A_i y_i).$$

For easy reference we record

$$\alpha y_i = 2 \sin \phi \begin{pmatrix} 0 \\ (-1)^i \sin \phi \\ \sin(\beta/2) \cos \phi \end{pmatrix}, \quad S = \begin{pmatrix} 1 & 0 & 0 \\ 0 & -1 & 0 \\ 0 & 0 & -1 \end{pmatrix}$$

and

$$A_2 = A_1^t = \zeta_1^{-1} \zeta_2 = \begin{pmatrix} 1 - 2 \cos^2(\beta/2) \cos^2 \phi & -\sin \beta \cos^2 \phi & \cos(\beta/2) \sin(2\phi) \\ -\sin \beta \cos^2 \phi & 1 - 2 \sin^2(\beta/2) \cos^2 \phi & \sin(\beta/2) \sin(2\phi) \\ -\cos(\beta/2) \sin(2\phi) & -\sin(\beta/2) \sin(2\phi) & -\cos(2\phi) \end{pmatrix}.$$

Using the notation $[z]_3 := z \cdot \epsilon_3$ and elementary computations based on the above gives:

Proposition 9. *The return map in the coordinate system defined by Φ_1 has the form*

$$T_2 T_1(x, y) = (x + [A_1(x - \alpha y_1)]_3 V(y), S A_1^t S A_1 y),$$

where

$$V(y) = \frac{[y]_3 A_1^t S A_1 y - [A_1^t S A_1 y]_3 y}{[A_1 y]_3 [A_1^t S A_1 y]_3}.$$

This vector satisfies: $[V(y)]_3 = 0$ and $V(y_1) = 0$. In particular, $T_2 T_1(x, y_1) = (x, y_1)$ whenever (x, y_1) is in the domain of $T_2 T_1$.

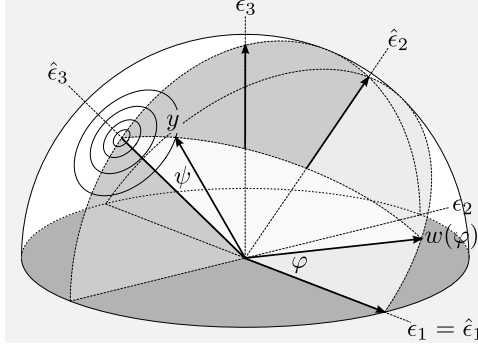


Figure 8: The velocity factor of orbits of the return billiard map $T_2 T_1$ in coordinate system Φ_1 lie in concentric circles with axis $y_1 = \hat{\epsilon}_3$. We use spherical coordinates φ and ψ relative to the axis $\hat{\epsilon}_3$ to represent the velocity $y \in S^2_+$. With respect to these coordinates, the return map sends $w(\varphi)$ to $w(\varphi + \theta)$, where θ is a function of the wedge angle α and the characteristic angle β of the no-slip reflection.

In order to study this return map in a neighborhood of (x, y_1) we use spherical coordinates about the axis y_1 :

$$(13) \quad y = \cos \psi y_1 + \sin \psi \cos \varphi \hat{\epsilon}_1 + \sin \psi \sin \varphi \hat{\epsilon}_2,$$

where

$$\hat{\epsilon}_1 := \epsilon_1, \quad \hat{\epsilon}_2 := \frac{1}{\sqrt{1 - \cos^2(\beta/2) \cos^2 \phi}} (\sin(\beta/2) \cos \phi \epsilon_2 + \sin \phi \epsilon_3), \quad \hat{\epsilon}_3 := y_1$$

form an orthonormal frame. See Figure 8. (Notice the typographical distinction between the corner angle ϕ of the wedge domain and the spherical coordinate φ .) Let

$$(X(x, \varphi, \psi), Y(x, \varphi, \psi)) := T_2 T_1(x, \cos \psi y_1 + \sin \psi \cos \varphi \hat{\epsilon}_1 + \sin \psi \sin \varphi \hat{\epsilon}_2)$$

and define

$$w := w(\varphi) := \cos \varphi \hat{\epsilon}_1 + \sin \varphi \hat{\epsilon}_2.$$

Thus we may write $y = \cos \psi (y_1 + \tan \psi w(\varphi))$. Since the rotation $S_2 := S A_1^t S A_1$ fixes y_1 , it acts on w as $S_2 w(\varphi) = w(\varphi + \theta)$ for some constant angle θ . It follows that

$$S_2 y = \cos \psi y_1 + \sin \psi w(\varphi + \theta).$$

The following proposition summarizes these observations and notations.

Proposition 10. *For points $y \in S_+^2$ in a neighborhood of y_1 we adopt spherical coordinates relative to the axis $y_1 = \hat{\epsilon}_3$, so that $y = \cos \psi (y_1 + \tan \psi w(\varphi))$ where*

$$w := w(\varphi) := \cos \varphi \hat{\epsilon}_1 + \sin \varphi \hat{\epsilon}_2.$$

See Figure 8. We also use the notations $[z]_3 := z \cdot \epsilon_3$, $S_1 := A_1^{-1} S A_1$, and $S_2 = S A_1^{-1} S A_1$. Let $R := T_2 T_1$ be the 2-step return map as defined above, whose domain contains a neighborhood of (x, y_1) for all $x \in \mathbb{R}^2$. Then $R(x, y_1) = (x, y_1)$ for all x and

$$R(x, y_1 + \tan \psi w(\varphi)) = (X, y_1 + \tan \psi S_2 w(\varphi)) = (X, \tan \psi w(\varphi + \theta))$$

for an angle θ , depending only on the wedge angle 2ϕ and the characteristic angle β of the no-slip reflection, such that

$$\begin{aligned} \cos \theta &= (S_2 \hat{\epsilon}_1) \cdot \hat{\epsilon}_1 = 1 - 8\delta^2 + 8\delta^4 \\ \sin \theta &= (S_2 \hat{\epsilon}_1) \cdot \hat{\epsilon}_2 = 4\delta(1 - 2\delta^2)\sqrt{1 - \delta^2}, \end{aligned}$$

where $\delta := \cos(\beta/2) \cos \phi$. Writing $(X, \Phi, \Psi) = R(x, \varphi, \psi)$ we have

$$(14) \quad R : \begin{cases} X &= x + \tan \psi \frac{[A_1(x - \gamma y_1)]_3}{[y_1]_3} \frac{(I + S_1)w - \frac{[(I + S_1)w]_3 y_1}{[y_1]_3} + \tan \psi \frac{[w]_3 S_1 w - [S_1 w]_3 w}{[y_1]_3}}{1 - \tan \psi \left(\frac{[(A_1 + S_1)w]_3}{[y_1]_3} - \tan \psi \frac{[A_1 w]_3 [S_1 w]_3}{[y_1]_3^2} \right)} \\ \Phi &= \varphi + \theta \\ \Psi &= \psi \end{cases}$$

Denoting $\mu_1 := \zeta_1^{-1} \epsilon_3 \in \mathbb{R}^2$, we further have $X(x + s\mu_1, \varphi, \psi) = X(x, \varphi, \psi) + s\mu_1$.

Since ψ remains constant under iterations of the return map $R = T_2 T_1$, we regard ψ as a fixed parameter. We are interested in small values of $r := \tan \psi$. Notice that $[A_1 z]_3 := (A_1 z) \cdot \epsilon_3 = z \cdot (A_1^t \epsilon_3) = \mu_0 \cdot z$, where

$$\mu_0 := A_1^t \epsilon_3 = \begin{pmatrix} \cos(\beta/2) \sin(2\phi) \\ \sin(\beta/2) \sin(2\phi) \\ -\cos(2\phi) \end{pmatrix}.$$

Write $x_0 := \alpha y_1$, so

$$x_0 = 2 \sin \phi \begin{pmatrix} 0 \\ -\sin \phi \\ \sin(\beta/2) \cos \phi \end{pmatrix}.$$

Then the proposition shows that R has the form

$$(15) \quad R : (x, \varphi) \mapsto (X = x + \mu_0 \cdot (x - x_0) V_r(\varphi), \Phi = \varphi + \theta),$$

where the vector $V_r(\varphi)$ can be made arbitrarily (uniformly) small by choosing ψ (or $r = \tan \psi$) sufficiently close to 0. Observe from the explicit form

$$V_r(\varphi) = \frac{1}{[y_1]_3} \frac{r \left((I + S_1)w - \frac{[(I + S_1)w]_3 y_1}{[y_1]_3} \right) + r^2 \frac{[w]_3 S_1 w - [S_1 w]_3 w}{[y_1]_3}}{1 - r \frac{[(A_1 + S_1)w]_3}{[y_1]_3} + r^2 \frac{[A_1 w]_3 [S_1 w]_3}{[y_1]_3^2}}$$

that $V_r(\varphi) \cdot \epsilon_3 = 0$ so that X is indeed in \mathbb{R}^2 .

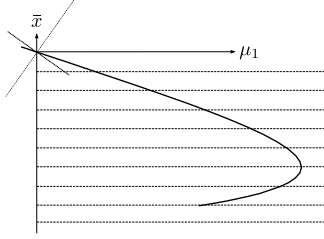


Figure 9: The map R sends fibers $x + \mathbb{R}\mu_1$ onto other such fibers preserving length. That is, $dR_{(x,\varphi)}\mu_1 = \mu_1$. The quotient is a measure preserving transformation on $\mathbb{R} \times \mathbb{T}^1$. The coordinate on the first factor of the quotient is $\bar{x} = x \cdot \mu_0$. The curve shown above is typical of the set to which orbits of R project in \mathbb{R}^2 .

Proposition 11. *The quantity $1 + \mu_0 \cdot V_r(\varphi)$ satisfies the coboundary relation*

$$(16) \quad 1 + \mu_0 \cdot V_r(\varphi) = \frac{\rho(\varphi)}{\rho(\varphi + \theta)},$$

where

$$\rho(\varphi) = 1 + r \frac{\tan \phi}{\sin(\beta/2)} \sin \varphi.$$

In fact, the transformation R on the 3-dimensional space $\mathbb{R}^2 \times \mathbb{R}/(2\pi\mathbb{Z})$, obtained by fixing a value of ψ (hence of $r = \tan \psi$), leaves invariant the measure

$$d\mu = c \left(1 + r \frac{\tan \phi}{\sin(\beta/2)} \sin \varphi \right) dA d\varphi,$$

where c is a positive constant (only dependent on the fixed parameters β, ψ, ϕ) and A is the standard area measure on \mathbb{R}^2 .

Proof. The canonical invariant measure on $\mathbb{R}^2 \times S_+^2$ has the form $y \cdot \epsilon_3 dA dA_S$, where A_S is the area measure on S_+^2 . For a fixed value of ψ we obtain an invariant measure on $\mathbb{R}^2 \times S^1$ of the form $y \cdot \epsilon_3 dA d\varphi$. Using the form of y given by (13), one obtains

$$y \cdot \epsilon_3 = \frac{\cos \psi \cos \phi \sin(\beta/2)}{\sqrt{1 - \cos^2(\beta/2) \cos^2 \phi}} \left(1 + r \frac{\tan \phi}{\sin(\beta/2)} \sin \varphi \right).$$

This shows that, up to a multiplicative constant, the invariant measure μ has the indicated form. Equation (16) is an easy consequence of the invariance of μ with respect to R . \square

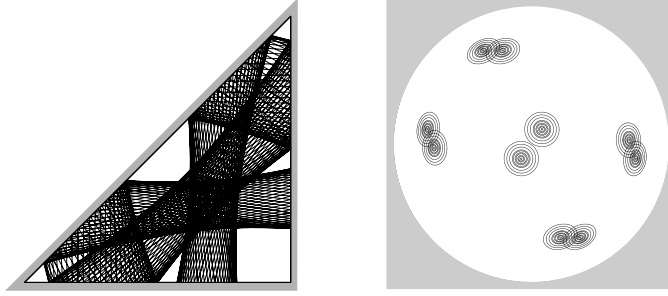


Figure 10: Projection to the plane of orbits in the neighborhood of a period-10 periodic orbit of a triangular no-slip billiard domain (left) showing typical stable behavior, along with the velocity phase portrait projections (right).

By using the coordinate system $(\bar{x}, \bar{y}) \mapsto \bar{x}\mu_0 + \bar{y}\mu_1$ on \mathbb{R}^2 , the area measure is $dA = d\bar{x} d\bar{y}$ and, as observed at the end of Proposition 10, the transformation R maps the fibers of the projection $(\bar{x}, \bar{y}) \mapsto \bar{x}$ to fibers preserving the length measure on fibers. Thus we obtain a transformation \bar{R} on $\mathbb{R} \times S^1$ preserving the measure $d\bar{\mu}(\bar{x}, \varphi) = \rho(\varphi) d\bar{x} d\varphi$ where $\rho(\varphi)$ has the stated expression. Using the quotient coordinates $\bar{x} = x \cdot \mu_0$ and ϕ and writing $V_r(\varphi) := V_r(\varphi) \cdot \mu_0$ we obtain

$$\bar{R}(\bar{x}, \phi) = ((1 + \bar{V}_r(\varphi))\bar{x} - \bar{x}_0 \bar{V}_r(\varphi), \phi + \theta).$$

In particular,

$$\bar{X} = \frac{\rho(\varphi)}{\rho(\varphi + \theta)} \bar{x} + \left(1 - \frac{\rho(\varphi)}{\rho(\varphi + \theta)} \right) \bar{x}_0.$$

The invariant measure is

$$d\bar{\mu}(\bar{x}, \varphi) = \rho(\varphi) d\bar{x} d\varphi$$

where $\rho(\varphi)$ is the density given in Proposition 11. It is now immediate that

$$\bar{R}^n(\bar{x}, \varphi) = \left(\frac{\rho(\varphi)}{\rho(\varphi + n\theta)} \bar{x} + \left(1 - \frac{\rho(\varphi)}{\rho(\varphi + n\theta)} \right) \bar{x}_0, \varphi + n\theta \right).$$

This shows that all the iterates of (\bar{x}, φ) remain uniformly close to the initial point for small values of ψ . Also notice that $(\zeta_1 \mu_0) \cdot e_{2,1} = \nu_2 \cdot e_{2,1} = \sin(2\phi) > 0$. This means that if \bar{x} remains bounded, the length coordinate along the base of \mathcal{P}_1 also must be similarly bounded. From this we conclude:

Corollary 12. *Assume the notation introduced at the beginning of this section. For all $q \in \mathcal{P}_i \setminus (\mathcal{P}_1 \cap \mathcal{P}_2)$, $i = 1, 2$, and any neighborhood \mathcal{V} of the period-2 state $(q, v_i) \in S_i^+$, there exists a small enough neighborhood $\mathcal{U} \subset \mathcal{V}$ of (q, v_i) the orbits of whose points remain in \mathcal{V} .*

Because any (bounded) polygonal billiard shape must have a corner with angle less than π , the following corollary holds.

Theorem 13. *Polygonal no-slip billiards cannot be ergodic for the canonical invariant measure.*

7 HIGHER ORDER PERIODIC ORBITS IN POLYGONS

The analysis of the previous section is based on the existence of period-2 orbits in wedge-shaped no-slip billiard tables. Existence of periodic orbits of higher periods presently seems difficult to establish analytically, although one such result for wedge domains will be indicated below in this section. This result strengthens an observation made in [8]. We first point out a generalization of Corollary 12 to perturbations of periodic orbits in general polygon-shaped domains.

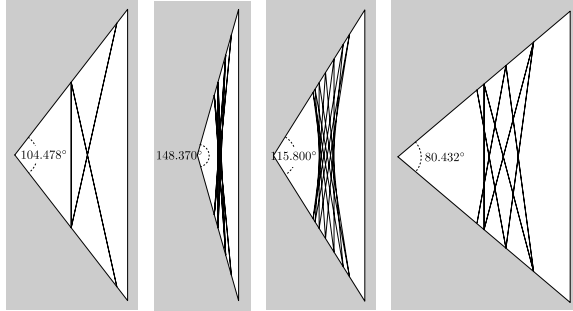


Figure 11: From left to right: projections to the plane of periodic orbits of periods 6, 14, 14, 14. (Bounded orbits in the same wedge domain are all periodic with the same period.) The rotation angle θ in each case is $2\pi p/q$ where $p/q = 1/3, 1/7, 2/7, 3/7$. Mass distribution of the disc particle is uniform.

Figure 10 illustrates the type of stability implied by the following Theorem 14.

Theorem 14. *Periodic orbits in no-slip polygon-shaped billiard domains are Lyapunov stable. That is, given an initial state $\xi_0 = (q_0, v_0)$ for a period- n orbit in such a billiard system, and for any neighborhood \mathcal{V} of ξ_0 , there exists a small enough neighborhood $\mathcal{U} \subset \mathcal{V}$ of ξ the orbits of whose elements remain in \mathcal{V} .*

Proof. The idea is essentially the same as used in the proof of Proposition 11 and Corollary 12. We only indicate the outline. By a choice of convenient coordinates around the periodic point, it is possible to show that the n -th iterate of the billiard map T , denoted $R := T^n$, can be regarded as a map from an open subset of $\mathbb{R}^2 \times S^1$ into this latter set, having the form $R(x, \varphi) = (x_0 + A(\varphi)(x - x_0), \varphi + \theta)$ for a certain angle θ , where $A(\varphi)$ is a linear transformation independent of x . Rotation invariance implies that R must satisfy the invariance property $R(x + su, \varphi) = R(x, \varphi) + su$ for a vector $u \in \mathbb{R}^2$. From this we define a map \bar{R} on (a subset of) the quotient $\mathbb{R} \times S^1$, $\mathbb{R}^2/\mathbb{R}u$. Furthermore, denoting by (\bar{x}, φ) the coordinates in this quotient space, invariance of the canonical measure implies invariance of a measure μ on this quotient having the form $d\mu(\bar{x}, \varphi) = \rho(\varphi) d\bar{x} d\varphi$. Invariance is with respect to the quotient map $\bar{R}(\bar{x}, \varphi) = (\bar{x}_0 + a(\varphi)(\bar{x} - \bar{x}_0), \varphi + \theta)$ for some function $a(\varphi)$. This function must then take the form $a(\varphi) = \rho(\varphi)/\rho(\varphi + \theta)$. Iterates of \bar{R} will then behave like the corresponding map for the wedge domain, defined prior to Theorem 12. \square

We turn now to the question of existence of periodic orbits of higher (necessarily even) periods for wedge shapes. Clearly, a necessary condition is that the angle θ introduced in Proposition 10 (see also Figure 8) be rational. For orbits that do not eventually escape to infinity, this is also a sufficient condition, as a simple application of Poincaré recurrence shows. (See [8].) Moreover, as θ is only a function of $\delta := \cos(\beta/2) \cos \phi$, which is given by (Proposition 10)

$$(17) \quad \cos \theta = 1 - 8\delta^2 + 8\delta^4,$$

where β is the characteristic angle of the system (a function of the mass distribution on the disc) and 2ϕ is the corner angle of the wedge domain, if a higher order periodic orbit exists for a given δ , all bounded orbits have the same period.

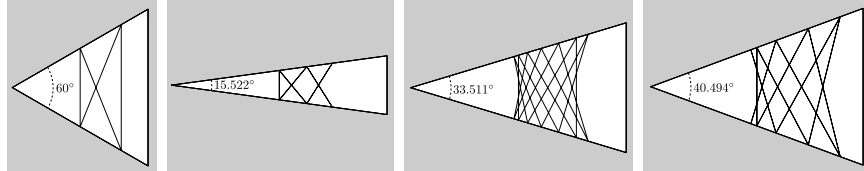


Figure 12: From left to right: projections of periodic orbits of periods 4, 10, 14, 18. The rotation angle θ in each case is $2\pi p/q$ where p/q is $1/2, 2/5, 3/7, 4/9$, respectively. Mass distribution is uniform.

We give a few examples for the uniform mass distribution, for which $\cos(\beta/2) = \sqrt{2/3}$. Solving 17 for $\cos \phi$, for $\theta = 2\pi p/q$, choosing first the negative square root, gives

$$(18) \quad \cos \phi_{p,q} := \frac{\sqrt{3}}{2} \sqrt{1 - \sqrt{\frac{1 + \cos(2\pi p/q)}{2}}}.$$

A few examples are shown in Figure 11.

Notice that there are no restrictions on the values of p and q . The following proposition is a consequence of these remarks.

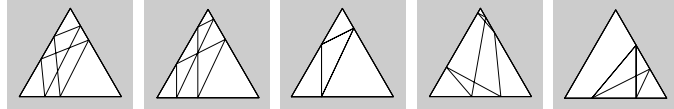


Figure 13: All orbits of an equilateral triangle no-slip billiard system are periodic with (not necessarily least) period equal to 4 or 6.

Theorem 15. *For any positive even integer n there exists a wedge domain for which the no-slip billiard has period- n orbits. More specifically, all bounded orbits of the no-slip billiard in a wedge domain with corner angle $\phi_{p,q}$ satisfying Equation 18 are periodic with period $2q$.*

Solving 17 for $\cos \phi$, for $\theta = 2\pi p/q$, but choosing now the positive square root, gives

$$\cos \phi_{p,q} := \frac{\sqrt{3}}{2} \sqrt{1 + \sqrt{\frac{1 + \cos(2\pi p/q)}{2}}}.$$

This makes sense so long as $0.392 \approx \arccos(-7/9)/2\pi \leq p/q \leq 0.5$, which greatly restricts the choices of p and q . A few examples in this case are shown in Figure 12.

It is interesting to observe that all orbits of the equilateral triangle are periodic with period 4 or 6. (See Figure 13 and [8] for the proof.) We do not know of any other no-slip billiard domain all of whose orbits are periodic.

8 LINEAR STABILITY IN THE PRESENCE OF CURVATURE

We now turn to the problem of characterizing stability of period-2 orbits for no-slip billiard domains whose boundary may have non-zero geodesic curvature. Here we only address *linear* rather than local stability. In other words, we limit ourselves to the problem of determining when the differential of the billiard map at a period-2 collision state $\xi = (q, v)$ is elliptic or hyperbolic, and obtaining sharp thresholds (where it is parabolic). A simple but key observation is contained in the following lemma.

Lemma 16. *Let $\xi = (q, v)$ be periodic with period 2 for the no-slip billiard map and consider the differential $\mathcal{T} := dT_\xi^2 : v^\perp \oplus v^\perp \rightarrow v^\perp \oplus v^\perp$. Then either all the eigenvalues of \mathcal{T} are real, of the form $1, 1, r, 1/r$ or, if not all real, they are $1, 1, \lambda, \bar{\lambda}$ where $|\lambda| = 1$.*

Proof. This is a consequence of the following observations. First, we know that $T^* \Omega = -\Omega$, where Ω is the canonical symplectic form (cf. Section 5). Therefore, the product of the eigenvalues of \mathcal{T} counted with multiplicity is 1. The vector (e_1, w_1) , where e_1 is the first vector in the product frame and w_1 is the first vector in the wavefront frame, is an

eigenvector for eigenvalue 1 of dT_ξ due to rotation symmetry, as already noted. If we regard dT_ξ as a self-map of $v^\perp \oplus v^\perp$ as in the corollary to Proposition 5 then we should use instead the vector (w_1, w_1) . (Recall that w_1 is collinear with the orthogonal projection of e_1 to v^\perp .) In addition, by reversibility of T , if λ is an eigenvalue of \mathcal{T} , then $1/\lambda$ also is, and since \mathcal{T} is a real valued linear map, the complex conjugates $\bar{\lambda}$ and $1/\bar{\lambda}$ are also eigenvalues. As the dimension of the linear space is 4, if one of the eigenvalues, λ , is not real, it must be the case that $\lambda = 1/\bar{\lambda}$ and we are reduced to the case $1, 1, \lambda, \bar{\lambda}$ with $\lambda\bar{\lambda} = 1$. If all eigenvalues are real, and $r \neq 1$ is an eigenvalue, then we are reduced to the case $1, 1, r, 1/r$. \square

Corollary 17. *The period-2 point ξ is elliptic for $\mathcal{T} = dT_\xi^2$ if and only if $|\text{Tr}(\mathcal{T}) - 2| < 2$.*

To proceed, it is useful to express the differential map of Corollary 6 in somewhat different form. First observe, in the period-2 case (in which $\tilde{v} = -v$ and $v^\perp = \tilde{v}^\perp$), that

$$w_2(\xi) = -w_2(\tilde{\xi}) \text{ and } \frac{\cos \psi(\tilde{q}, v)}{\cos \phi(\tilde{q}, v)} = \frac{\cos \psi(\tilde{\xi})}{\cos \phi(\tilde{\xi})} = \frac{\cos \psi(\xi)}{\cos \phi(\xi)}.$$

(See Section 3.) Now define the rank-1 operator

$$\Theta_{\tilde{\xi}}(Z) := 2 \cos(\beta/2) \frac{\cos \psi(\tilde{\xi})}{\cos \phi(\tilde{\xi})} \langle w_2(\tilde{\xi}), Z \rangle u_1(\tilde{q}).$$

Then

$$(19) \quad dT_\xi \begin{pmatrix} X \\ Y \end{pmatrix} = \begin{pmatrix} I & tI \\ -\kappa(\tilde{q})\Theta_{\tilde{\xi}} & C_{\tilde{q}} - t\kappa(\tilde{q})\Theta_{\tilde{\xi}} \end{pmatrix} \begin{pmatrix} X \\ Y \end{pmatrix}.$$

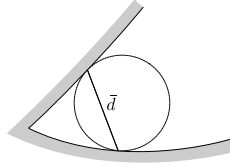


Figure 14: For a billiard domain with piecewise smooth boundary, arbitrarily near any corner with inner angle less than π , there are linearly stable period-2 orbits.

When $\kappa(q) = \kappa(\tilde{q})$ there is a simplification in the criterion for ellipticity, as will be seen shortly. With this special case in mind we define the linear map R_ξ on v^\perp by $R_\xi w_i(\xi) = -(-1)^i w_i(\xi)$, $i = 1, 2$. Notice that $R u_1(q) = u_1(\tilde{q})$. Then

$$R_{\tilde{\xi}} C_{\tilde{q}} = C_q R_\xi, \quad R_{\tilde{x}} \Theta_{\tilde{\xi}} = \Theta_\xi R_\xi.$$

The same notation R_ξ will be used for the map on $v^\perp \oplus v^\perp$ given by $(z_1, z_2) \mapsto (R_\xi z_1, R_\xi z_2)$. Then $R := R_\xi = R_{\tilde{\xi}}$ since $w_i(\tilde{\xi}) = -(-1)^i w_i(\xi)$. It follows that

$$(20) \quad RdT_\xi R = \begin{pmatrix} I & tI \\ -\kappa(\tilde{q})\Theta_\xi & C_q - t\kappa(\tilde{q})\Theta_\xi \end{pmatrix}.$$

In particular, when $\kappa(q) = \kappa(\tilde{q})$, we have $RdT_\xi R = dT_{\tilde{\xi}}$ and $dT_\xi^2 = (dT_{\tilde{\xi}})^2$. Therefore, rather than computing the trace of dT_ξ^2 , we need only consider the easier to compute trace of RdT_ξ . The result is recorded in the next lemma.

Lemma 18. *Let $\xi = (q, v)$ have period 2 and set $\tilde{\xi} := T(\xi)$, $C := C_q$, $\Theta := \Theta_q$. Then*

$$\text{Tr}(dT_\xi^2) = \text{Tr}\{I + (CR)^2 - t(\kappa(q) + \kappa(\tilde{q}))[\Theta + (CR)(\Theta R)] + t^2\kappa(q)\kappa(\tilde{q})(\Theta R)^2\}.$$

When $\kappa := \kappa(\tilde{q}) = \kappa(q)$, we have $\text{Tr}(RdT_\xi) = \text{Tr}(CR + t\kappa\Theta)$.

Proof. These expressions follow easily given the above definitions and notations. \square

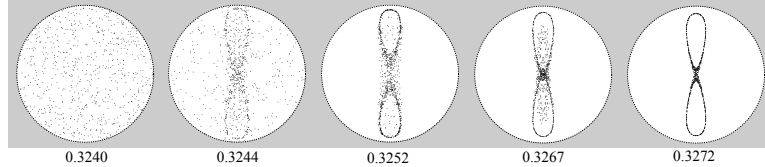


Figure 15: Velocity phase portraits of single orbits near the periodic orbit of the no-slip Sinai billiard corresponding to $\phi = 0$. The mass distribution is uniform. The numbers are the radius of the circular scatterer.

The traces can now be computed using Equations (3) and (4). The matrices expressing C, R, Θ in the wavefront basis of v^\perp are given as follows. For convenience we write

$$c := \cos(\beta/2), \quad c_\phi := \cos\phi, \quad c_\psi := \cos\psi, \quad \varrho := \sqrt{1 - \cos^2(\beta/2)\cos^2\phi},$$

where $\phi = \phi(\xi)$ and $\psi = \psi(\xi)$ are defined in Corollary 6.

$$[C]_w = \begin{pmatrix} 1 - 2c^2c_\phi^2 & -2cc_\phi\varrho \\ -2cc_\phi\varrho & -1 + 2c^2c_\phi^2 \end{pmatrix}, \quad [R] = \begin{pmatrix} 1 & 0 \\ 0 & -1 \end{pmatrix}, \quad [\Theta]_w = 2c\frac{c_\psi}{c_\phi} \begin{pmatrix} 0 & \varrho \\ 0 & -cc_\phi \end{pmatrix}.$$

Let \bar{d} be the distance between the projections of q and \tilde{q} on plane the billiard table, \bar{v} the projection of v on the same plane and t , as before, the time between consecutive collisions. From $\cos\psi = \sin(\beta/2)\cos\phi/\sqrt{1 - \cos^2(\beta/2)\cos^2\phi}$ it follows that $t\cos\psi = \cos\phi\bar{d}$.

We then obtain

$$(21) \quad \text{Tr}(RdT_\xi) = \text{Tr}(CR) + t\kappa\text{Tr}(\Theta) = 2[1 - 2\cos^2(\beta/2)\cos^2\phi] - 2\kappa\bar{d}\cos^2(\beta/2)\cos\phi$$

and

$$(22) \quad \begin{aligned} \text{Tr}(dT_\xi^2) = 4 & \left\{ [1 - 2\cos^2(\beta/2)\cos^2\phi]^2 \right. \\ & - (\kappa(q) + \kappa(\tilde{q}))\cos^2(\beta/2)\cos\phi[1 - 2\cos^2(\beta/2)\cos^2\phi]\bar{d} \\ & \left. + \kappa(q)\kappa(\tilde{q})\bar{d}^2\cos^4(\beta/2)\cos^2\phi \right\}. \end{aligned}$$

Observe that in the special case in which $\kappa(q) = \kappa(\tilde{q})$ we have

$$\text{Tr}(dT_\xi^2) = \{2[1 - 2\cos^2(\beta/2)\cos^2\phi] - 2\kappa\bar{d}\cos^2(\beta/2)\cos\phi\}^2.$$

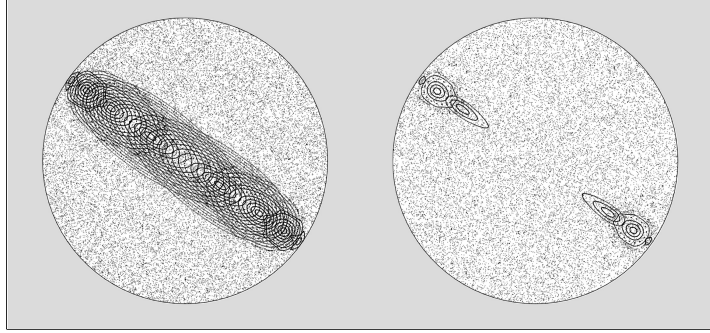


Figure 16: On the left: velocity phase portrait of the no-slip Sinai billiard with scatterer radius $R = 0.35$. Since this is greater than the transition value $R = 1/3$, the period-2 orbits parametrized by ϕ are all elliptic. On the right, $R = 0.32$ and ellipticity has been destroyed for orbits with smaller values of ϕ . No matter how small R is, elliptic orbits always exist for ϕ sufficiently close to $\pi/2$.

Theorem 19. *Suppose that the billiard domain has a piecewise smooth boundary with at least one corner having inner angle less than π . Then, arbitrarily close to that corner point, the no-slip billiard has (linearly) elliptic period-2 orbits.*

Proof. Period-2 orbits exist arbitrarily close to the corners of a piecewise smooth billiard domain as Figure 14 makes clear. For period-2 orbits near a corner the above expression for $\text{Tr}(dT_\xi^2)$ gives for small \bar{d}

$$0 < \text{Tr}(dT_\xi^2) = 4 \left[1 - 2 \cos^2(\beta/2) \cos^2 \phi \right]^2 + O(\bar{d}) < 4.$$

This implies that

$$|\text{Tr}(dT_\xi^2) - 2| < 2$$

and the theorem follows from Corollary 17. \square

Theorem 19 (and numerical experiments) strongly suggests that such no-slip billiards will always admit small invariant open sets and thus cannot be ergodic with respect to the canonical billiard measure.

We illustrate numerically the transition between elliptic and hyperbolic in the special case of equal curvatures at q and \tilde{q} . Define $\zeta := \kappa\bar{d}$. When $\zeta > 0$ (equivalently, the curvature is positive), the critical value of ζ is

$$\zeta_0 = \frac{2 - 2 \cos^2(\beta/2) \cos^2 \phi}{\cos^2(\beta/2) \cos \phi}.$$

The condition for ellipticity is $\zeta > \zeta_0$. When $\zeta < 0$, the critical value of ζ is

$$\zeta_0 = -2 \cos \phi$$

and the condition for ellipticity is $|\zeta| < |\zeta_0|$.

Consider the example of the no-slip Sinai billiard. (See Figures 3 and 6.) We examine small perturbations of the periodic orbit corresponding to the angle $\phi = 0$. Figure 15 suggests a transition from chaotic to more regular type of behavior for a radius between 0.32 and 0.33. In reality the critical radius for the $\phi = 0$ periodic orbits is exactly 1/3. So the observed numbers are smaller. We should bear in mind that the periodic points are not isolated, but are part of a family parametrized by ϕ . As ϕ increases, the critical parameter ζ_0 changes (for the uniform mass distribution, where $\cos^2(\beta/2) = 2/3$) according to the expression $\zeta_0 = (3 - \cos^2 \phi)/\cos \phi$. Given in terms of the radius of curvature, $\zeta = (1 - 2R \cos \phi)/R$. Solving for the critical R yields $R_0 = \frac{\cos \phi}{3}$. Thus for a period-2 trajectory having a small but non-zero ϕ , the critical radius is less than 1/3. It is then to be expected that the experimental critical value of R , for orbits closed to that having $\phi = 0$ will give numbers close to but less than 1/3. Moreover, as R_0 approaches 0 when ϕ approaches $\pi/2$, we obtain the following proposition which, together with experimental evidence indicates that the no-slip Sinai billiard is not ergodic.

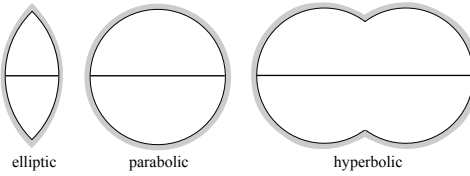


Figure 17: Family of focusing no-slip billiards.

Proposition 20. *The no-slip Sinai billiard, for any choice of scatterer curvature, will contain (linearly) elliptic periodic trajectories of period 2.*

As another example, consider the family of billiard regions bounded by two symmetric arcs of circle depicted in Figure 17.

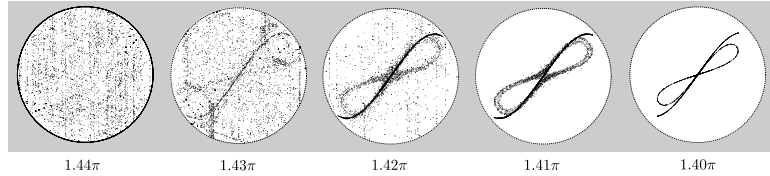


Figure 18: The indicated number is the angle of the circular cap. Each depicted orbit is a perturbation of the horizontal period-2 orbit at the middle height, as shown in Figure 17. Apparent chaotic behavior occurs for an angle much greater than π . This is expected since the parallel period-2 orbits remain linearly stable as the angle cap increases, up to a point.

In this case, the critical transition from hyperbolic to elliptic, for the horizontal periodic

orbit at middle height shown in the figure, happens for the disc. A transition behavior similar to that observed for the Sinai billiard seems to occur near the period-2 orbits shown in Figure 17. The number indicated below each velocity phase portrait is the angle of each circular arc. Thus, for example, the disc corresponds to angle π ; smaller angles give shapes like that on the left in Figure 17. The cut-off angle at which the indicated periodic orbit becomes elliptic is π . Notice, however, that the experimental value for this angle is greater than π . Just as in the Sinai billiard example, we should keep in mind that the periodic orbits are not isolated; in this case, the bias would be towards greater values of the angle.

9 FINAL REMARK

Of the results discussed above, the more definite ones apply to polygonal no-slip billiards; they imply a strong stability of periodic orbits. For general curvature, we also noted above that elliptic behavior is very common and hard to destroy.

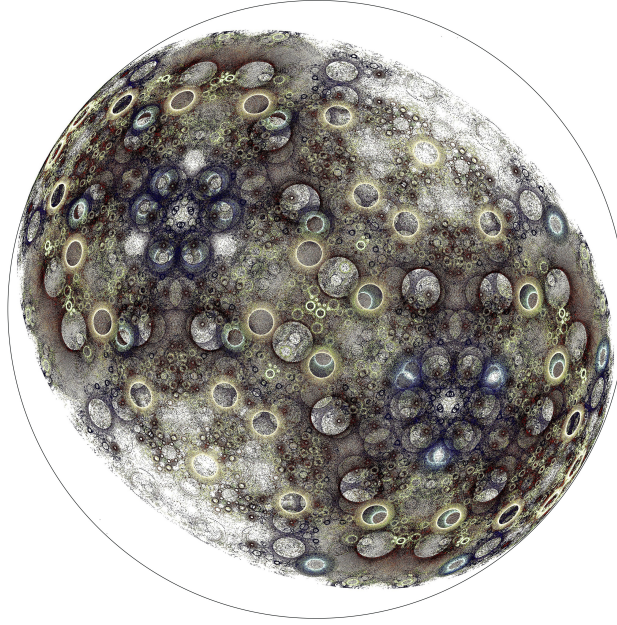


Figure 19: Velocity phase portrait of the no-slip billiard on a regular pentagon. Orbits all seem to lie in a stable neighborhood of some periodic orbit.

A more striking general picture for polygonal billiards, which we cannot yet validate analytically or even clearly formulate, is suggested by numerical experiments. Figure 19, which is very typical of polygonal billiards, represents a partially filled velocity phase portrait for the no-slip billiard on a regular pentagon. The orbits drawn all seem to lie on

a stable neighborhood of some periodic orbit, and this pattern is seen at all scales that we have explored, but we do not yet have a precise topological-dynamics description of this observation.

Acknowledgement: H.-K. Z. was partially supported by NSF grant DMS-1151762 and a grant from the Simons Foundation (337646, HZ).

REFERENCES

- [1] D.S. Broomhead, E. Gutkin, *The dynamics of billiards with no-slip collisions.* Physica D 67 (1993) 188-197.
- [2] L.A. Bunimovich, *The ergodic properties of certain billiards.* Funkt. Anal. Prilozh. 8 (1974) 73-74.
- [3] L. A. Bunimovich, *Mushrooms and other billiards with divided phase space.* Chaos, 11 (2001) 802-808.
- [4] N. Chernov, R. Markarian, *Chaotic billiards.* Mathematical Surveys and Monographs, V. 127, American Mathematical Society, 2006.
- [5] M. F. Correia, H. K. Zhang, *Stability and ergodicity of moon billiards.* Chaos, 25 083110 (2015).
- [6] M. Correia, C. Cox, H.-K. Zhang, *Ergodicity in umbrella billiards,* New Horizons in Mathematical Physics, Vol. 1, No. 2, September 2017, pp. 56-67.
- [7] C. Cox, R. Feres, *Differential geometry of rigid bodies collisions and non-standard billiards.* Discrete and Continuous Dynamical Systems-A, 33 (2016) no. 11, 6065-6099.
- [8] C. Cox, R. Feres, *No-slip billiards in dimension 2.* Dynamical Systems, Ergodic Theory, and Probability: in Memory of Chernov, Contemporary Mathematics, vol. 698, Amer. Math. Soc., p. 91-110 (2017)
- [9] R.L. Garwin, *Kinematics of an Ultraelastic Rough Ball.* American Journal of Physics, V. 37, N. 1 January 1969, pages 88-92.
- [10] V. Kaloshin, J.N. Mather, E. Valdinoci, *Instability of Resonant Totally Elliptic Points of Symplectic Maps in Dimension 4.* Analyse complexe, systèmes dynamiques, sommabilité des séries divergentes et théories galoisiennes. II. Astérisque 297, 79-116 (2004)
- [11] H. Larralde, F. Leyvraz, and C. Mejía-Monasterio, *Transport properties of a modified Lorentz gas.* J. Stat. Phys. 113, 197-231 (2003).
- [12] J. Moser, *On invariant curves of area-preserving mappings of an annulus.* Nachr. Akad. Wiss. Göttingen No.1 (1962).

- [13] C. Mejía-Monasterio, H. Larralde, and F. Leyvraz, *Coupled Normal Heat and Matter Transport in a Simple Model System*, Physical Review Letters, V. 86, N. 24, 5417-5420 (2001).
- [14] I. Niven, *Irrational Numbers*, Wiley, 1956, p. 41.
- [15] Y. G. Sinai, *Dynamical systems with elastic reflections. Ergodic properties of dispersing billiards*. Uspehi Mat. Nauk 25 (1970), no. 2 (152), 141-192.
- [16] S. Tabachnikov, *Billiards*, in Panoramas et Synthèses 1, Société Mathématique de France, 1995.
- [17] M.B. Sevryuk, *Reversible Systems*, Lecture Notes in Mathematics 1211, Springer 1986.
- [18] M.B. Sevryuk, *Lower dimensional tori in reversible systems*. Chaos, 1 (1991) 160-167.
- [19] M. Wojtkowski, *The system of two spinning disks in the torus*. Physica D 71 (1994) 430-439.